DALTON
FULL PAPER

In situ syntheses of *trans*-spanned octahedral ruthenium complexes. Crystal structures of *trans*-[Ru(Cl)(trpy){$Ph_2PC_6H_4CH_2O(CO)(CH_2)_4(CO)OCH_2C_6H_4PPh_2$}][$PF_6$]·0.25$C_6H_5Me$·0.5$CH_2Cl_2$ and *trans*-[Ru(Cl)(trpy)(PPh_3)$_2$][BF_4]·CH_2Cl_2 †

Willie J. Perez,[a] Charles H. Lake,[a] Ronald F. See,[a] Laurence M. Toomey,[a] Melvyn Rowen Churchill,[a] Kenneth J. Takeuchi,*[a] Christopher P. Radano,[b] Walter J. Boyko[b] and Carol A. Bessel*[b]

[a] *Department of Chemistry, Natural Sciences Complex, State University of New York at Buffalo, Buffalo, NY 14260, USA*
[b] *Department of Chemistry, Villanova University, 800 Lancaster Ave., Villanova, PA 19085, USA*

Received 29th September 1998, Accepted 21st May 1999

The formation of stable, undistorted octahedral transition metal complexes which contain a *trans*-spanning bidentate ligand remains a synthetic challenge. The reported complexes are of the type *trans*-[Ru(Cl)(trpy){$Ph_2PC_6H_4CH_2O(CO)Y(CO)OCH_2C_6H_4PPh_2$}][$PF_6$] [where trpy = 2,2′ : 6′,2″-terpyridine and Y = $(CH_2)_3$ = C3SPAN, **6**; $(CH_2)_4$ = C4SPAN, **7**; or isophthalate = ISPAN, **8**] and represent the first examples of *trans*-spanned transition metal complexes which display little bond angle distortion from octahedral geometry and also contain a bridging linkage which is stable towards oxidation, reduction and hydrolysis. These complexes were characterized by elemental analyses, cyclic voltammetry, conductivity and UV-VIS spectroscopy. COSY, HETCOR and variable temperature (^{1}H and ^{13}C) NMR spectra of the complexes are consistent with a flexible spanning linkage that does not demonstrate restricted rotation about either the P–C_{ipso} or the Ru–P bonds while the X-ray crystal structure analysis of **7** showed that the spanning linkage is positioned to one side of the meridional chloride.

The formation of stable, undistorted octahedral transition metal complexes which contain a *trans*-spanning bidentate ligand presents a synthetic challenge in several respects.[1,2] To date, *trans*-spanning bidentate ligands have been prepared by two distinct methods: the synthesis of a bidentate ligand and its subsequent coordination to the transition metal center (preformed ligand strategy), and the bonding of two monodentate ligands to the metal center followed by the joining of the ligands with a *trans*-spanning linkage (*in situ* ligand strategy).

The preformed ligand strategy has been used effectively by Shaw and coworkers as they prepared several series of large ring complexes of the general formula *trans*-[$M(Cl)_2${$Bu_2P(CH_2)_nPBu_2$}] (M = Pd or Pt; n = 5–10),[3–5] or *trans*-[{$M(Cl)_2[Bu_2P(CH_2)_nPBu_2]$}$_x$] (M = Pd or Pt, n = 8, 9, 10 or 12; x = 1–3)[6–9] where each complex contained a flexible diphosphine ligand. Initially, Shaw and coworkers proposed that the presence of the bulky *tert*-butyl groups attached to the phosphorus donor atoms resulted in repulsive interactions between the substituents favoring a *trans*-geometry. Alcock[10–12] and McAuliffe[13–17] later prepared a number of *trans*-spanning Rh, Ni, Pt and Pd complexes with bis(diphenylphosphino)ethers, bis(diphenylphosphino)alkanes and bis(dimethylarsino)alkanes suggesting that the length of the spanning ligand was a large contributor to obtaining the *trans*-geometry. This argument was in agreement with those of McAuliffe[17] and others[18] who prepared ligands with both methyl, ethyl or phenyl substituents on the pnictogen or chalcogen donor atoms. In addition to preformed bidentate ligands with flexible chains, Venanzi and coworkers[19–26] and others[27] demonstrated the use of bis(dialkyl or diaryl phosphinomethyl)benzophenanthrene ligands as rigid *trans*-spanning "spacers." These rigid ligands have been used to span distorted trigonal, pseudo-tetrahedral, square planar, square pyramidal and octahedral metal centers.

While the preformed ligand strategy has been successful, it is not without limitations. First, the successful *trans*-positioning of preformed spanning ligands with flexible backbones can be crucially dependent on the choice of starting material. For example, in the preparation of $PtCl_2[Ph_2As(CH_2)_nAsPh_2]$ (n = 6–12, 16), the use of the starting material K_2PtCl_4 leads to the formation of the *cis* isomer, the use of $K[PtCl_3(H_2C{=}CH_2)]$ leads to the formation of the *trans* isomer, and the use of $Pt(C_6H_5CN)_2Cl_2$ leads to the formation of a *cis–trans* mixture.[17c] This marked dependency on the starting material makes the rational and systematic design of *trans*-spanned complexes difficult. Second, the use of preformed ligands can result in dimerization when the preformed ligands can bridge between two metal centers.[16,17d,18,23,28] This behavior was observed for [Pt{$Ph_2As(CH_2)_nAsPh_2$}Cl_2] (n = 6–12, 16) where both *trans* monomers and *cis* dimers were formed,[17d] as well as for [$PtCl_2${$Ph_2P(CH_2)_nPPh_2$}] complexes where both *cis* and *trans* monomers and *cis* and *trans* dimers were formed.[16] A third limitation is that preformed ligands with flexible backbones can form cyclometallated complexes[28–37] such as [IrH(Cl)($Bu_2PCH_2CH_2CHCHRCH_2PBu_2$)], where the *C* forms an iridium–carbon bond.[29] Such cyclometallation products are often observed with square planar or trigonal bipyramidal geometries. A fourth limitation is that the preformed rigid spanning ligands can cause strain which produces transition metal complex geometries distorted from octahedral geometry. The strain caused by the bis(diphenylphosphinomethyl)benzo[*c*]phenanthrene ligand (SL1) is evident in complexes of the type [M(SL1)]X or [M(SL1)X] where Venanzi reported that the P–M–P angle ranges from 132° for Cu to 141° for Ag, to 176° for Au.[20]

† *Supplementary data available*: NMR spectra. Available from BLDSC (No. SUP 57568, 19 pp.). See Instructions for Authors, 1999, Issue 1 (http://www.rsc.org/dalton).

The second method for formation of complexes with a *trans*-spanning bidentate ligand is the *in situ* ligand strategy. Using this strategy, Takeuchi and coworkers synthesized *trans*-spanning octahedral complexes of the form $[Ru(Cl)(trpy)(SL2)]^+$ [trpy = 2,2′:6′,2″-terpyridine and $SL2 = Ph_2PC_6H_4CH_2N(Me)(CH_2)_nN(Me)CH_2C_6H_4PPh_2$ or $Ph_2PC_6H_4CH_2N(Me)_2(CH_2)_nN(Me)_2CH_2C_6H_4PPh_2$; $n = 5$ or 6] by linking two coordinated *trans*-positioned tertiary phosphine ligands with a diamine.[38] These complexes were the first reported cases of *in situ* generated, *trans*-spanning ligands on an octahedral metal center where the spanning ligand bridged over the *cis* coordinated meridional chloride ligand. Like the preformed ligand strategy, the *in situ* ligand strategy offered flexibility in terms of both backbone length and composition. In addition, with the *in situ* ligand strategy the major reaction product was the *trans*-spanned complex and no cyclometallated complex was found. Disadvantages in the *in situ* strategy resulted from the use of the amine linkages. In the *trans*-spanned complex, the tertiary amine linkages were readily oxidized and evidence for dealkylation of the quaternary amine linkages was observed. To overcome these disadvantages, we developed a new ligand system that retained the benefits of the *in situ* ligand strategy while producing a ligand that is stable to oxidation and reduction.

In this work we report the formation of $[Ru(Cl)(trpy)(L)]^+$ [where $L = Ph_2PC_6H_4CH_2O(CO)Y(CO)OC_6H_4PPh_2$ and Y = $(CH_2)_3$ = C3SPAN, **6**; $(CH_2)_4$ = C4SPAN, **7**; and isophthalate = ISPAN, **8**]. The use of the *in situ* strategy with an ester linkage retains the span versatility in both length and structure, while making the span stable against degradation by oxidation and reduction. Additionally, decomposition due to hydrolysis is not observed on exposure of the complexes to either mildly acidic or basic solutions (pH = 2 to 10). Finally, the new *trans*-spanning complexes display good solubility in organic solvents, which facilitated the collection of variable temperature NMR spectra and the formation of single crystals suitable for X-ray diffraction studies.

Experimental

Materials

$RuCl_3 \cdot nH_2O$ was obtained on loan or purchased from Johnson Matthey/Alfa/Aesar. 2,2′:6′,2″-Terpyridine was purchased from G. F. Smith Chemical Company or was synthesized by literature methods.[39] Triphenylphosphine was purchased from Aldrich Chemical Company or Strem Chemical. Methylene chloride (J. T. Baker) was dried over activated 5 Å molecular sieves and distilled under N_2.[40] All other solvents and materials were of reagent quality and were used as received. Reactions were conducted under a nitrogen atmosphere unless otherwise noted.

Measurements

Elemental analyses were performed by Atlantic Microlabs, Norcross, GA. UV-VIS spectra were recorded using a Bausch and Lomb Spectronic 2000, a Milton Roy Spectronic 3000 Diode Array Spectrophotometer, or a Cary 1G UV-VIS Spectrophotometer. Conductivity measurements were performed in acetonitrile using a YSI Model 31 conductivity bridge.

Electrochemical measurements were made *versus* a saturated sodium chloride calomel reference electrode (SSCE) using either an IBM EC/225 voltammetric analyzer, a PAR Model 173 Potentiostat/Galvanostat equipped with a PAR Model 175 Universal Programmer or a BAS CV-50W Voltammetric Analyzer. A platinum disc working electrode was used along with a platinum wire common electrode. Electrochemical measurements used 0.1 M tetrabutylammonium tetrafluoroborate (TBAB) as the electrolyte and were conducted with ferrocene ($E_{1/2}$ = +0.40 V *vs*. SSCE in CH_3CN, $E_{1/2}$ = +0.50 V *vs*. SSCE in CH_2Cl_2) as the internal standard.

All NMR spectra were obtained on a Varian XL-300 spectrometer in CD_2Cl_2. ^1H spectra were obtained at 299.9 MHz and referenced to tetramethylsilane. ^{13}C spectra were obtained at 75.4 MHz and referenced to CD_2Cl_2 (δ 53.8). Proton–proton COSY and carbon–hydrogen HETCOR were run with standard Varian-supplied pulse sequences. The one-bond HETCOR direct detection sequence utilized BIRD pulses[41] to suppress proton–proton couplings in the f_1 domain of the 2D maps. Quaternary carbon resonances in trpy were assigned using the Varian-supplied direct detection HETCOR sequence (no BIRD pulse) optimizing defocussing/refocussing delays for the appropriate $''J_{C-H}$ constants. Several sets of delays were used near each desired *J*-value in order to avoid loss of the appropriate correlation signals due to one-bond modulation of the long-range response intensity.[42]

Crystallography

Data collection. Crystals were aligned on a Siemens-upgraded Syntex $P2_1/R3$ diffractometer equipped with a highly-oriented graphite crystal monochromator. The determination of the Laue symmetry, crystal class, unit-cell parameters and the crystal orientation matrix were carried out by previously described techniques.[43] Room-temperature data were collected with Mo-Kα radiation (λ = 0.71073 Å), using the θ–2θ scan technique for **7**, and the ω scan technique for **5** where peak overlap was a possible problem. Details of the data collection are in Table 1. All reflections in each data set were corrected for Lorentz and polarization effects and for absorption (semi-empirical).

Solution and refinement of the structures. All crystallographic calculations were carried out on a VAX3100 workstation with the use of the Siemens SHELXTL PLUS[44] program set. The analytical scattering factors for neutral atoms were corrected for both the $\Delta f'$ and the $i\Delta f''$ components of anomalous dispersion. The structures were solved by a combination of direct methods and Fourier-difference techniques. All non-hydrogen atoms were refined anisotropically, and hydrogen atoms were included in calculated positions with d(C–H) = 0.96 Å.[45] Details of each structure solution and its refinement may be found in Table 1. A diagram of one structure was generated using ORTEP II.[46]

CCDC reference number 186/1479.

Preparations

The complexes $RuCl_3(trpy)$,[47] *trans*-$[Ru(Cl)_2(trpy)\{Ph_2PC_6H_4(CH_2OC_5H_9O)$-*p*$\}]$, **1**,[38] *cis*-$[Ru(Cl)_2(trpy)\{Ph_2PC_6H_4(CH_2OC_5H_9O)$-*p*$\}]$, **2**,[38] *trans*-$[Ru(Cl)(trpy)\{Ph_2PC_6H_4(CH_2OC_5H_9O)$-*p*$\}_2][PF_6]$, **3**,[38] *trans*-$[Ru(Cl)(trpy)\{Ph_2PC_6H_4(CH_2OH)$-*p*$\}_2][PF_6]$, **4**,[38] and *trans*-$[Ru(Cl)(trpy)(PPh_3)_2]^+$, **5**,[47] were synthesized following published procedures.

***trans*-[Ru(Cl)(trpy)(C3SPAN)][PF$_6$], 6.** A 0.174 g (0.158 mmol) sample of **4** was dissolved in 17 mL of CH_2Cl_2 and the solution was outgassed with N_2 for 5 min. Glutaryl dichloride (0.027 mL, 0.21 mmol) was added and the reaction mixture was heated to reflux for 24 h. After cooling, the volume of the solution was reduced to dryness on a rotary evaporator. The residue was redissolved in CH_2Cl_2 and purified by passing through an alumina column using 100:1 (v/v) CH_2Cl_2–MeOH as the eluent. The first tan-orange band was collected and the solution was reduced to dryness with a rotary evaporator. The product was redissolved in a minimal amount of CH_2Cl_2 and precipitated by dropwise addition to Et_2O (*ca.* 100 mL). The solid was collected by vacuum filtration, washed with a minimum amount of Et_2O and air dried. A 0.111 g (0.093 mmol, 59% yield) sample of yellow-brown product was obtained (Calc. for $C_{58}H_{49}ClF_6N_3O_4P_3Ru \cdot 2H_2O$: C, 56.57; H, 4.02. Found: C, 56.58; H, 4.13%).

Table 1 Details of X-ray diffraction studies of *trans*-[Ru(Cl)(trpy)(PPh_3)$_2$][BF_4]·CH_2Cl_2 **5** and *trans*-[Ru(Cl)(trpy)(C4SPAN)][PF_6]·0.25C_6H_5Me·CH_2Cl_2 **7**

	5	**7**
Formula	$C_{51}H_{41}ClN_3P_2BF_4Ru·CH_2Cl_2$	$C_{59}H_{51}ClO_4N_3P_3F_6Ru·0.25C_6H_5Me·0.5CH_2Cl_2$
M	1066.1	1275
Crystal system	Monoclinic	Triclinic
Space group	$P2_1/c$	$P\bar{1}$
a/Å	17.8306(38)	10.9656(18)
b/Å	12.7954(26)	13.9782(22)
c/Å	21.7707(40)	19.8449(26)
α/°	90.00	89.212(12)
β/°	104.195(15)	85.938(12)
γ/°	90.00	68.071(12)
U/Å^3	4815.4(1.7)	2814.4(7)
Z	4	2
D_c/Mg m^{-3}	1.470	1.505
μ(Mo-Kα)/mm^{-1}	0.606	0.529
Independent reflections	6329	7391
Reflections > 6σ(F)	3118	4070
Final R indices (all data): R, wR	0.063, 0.038	0.092, 0.076
Final R indices (6σ data): R, wR	0.049, 0.035	0.044, 0.046

***trans*-[Ru(Cl)(trpy)(C4SPAN)][PF_6], 7.** A 0.101 g (0.0916 mmol) sample of **4** was dissolved in 7.2 mL of CH_2Cl_2. Adipoyl dichloride (0.020 mL; 0.14 mmol) was added and the reaction mixture was heated to reflux for 4 h. The reaction mixture was reduced to dryness with a rotary evaporator. The residue was passed through an alumina column using a 150:1 (v/v) CH_2Cl_2–MeOH solution as the eluent. The first tan-orange band was collected and reduced to dryness with a rotary evaporator. This residue was redissolved in a minimum amount of CH_2Cl_2 and precipitated by dropwise addition to toluene. The yellow-brown product was collected by vacuum filtration, washed with Et_2O and air dried; yield 0.067 g (0.055 mmol); 59% (Calc. for $C_{59}H_{51}ClF_6N_3O_4P_3Ru·C_6H_5Me$: C, 60.90; H, 4.56. Found: C, 60.57; H, 4.62%).

***trans*-[Ru(Cl)(trpy)(ISPAN)][BF_4], 8.** A 0.100 g (0.0907 mmol) sample of **4** was dissolved in 7.0 mL of CH_2Cl_2. Isophthaloyl dichloride (0.022 g; 0.11 mmol) was added and the reaction mixture was heated to reflux for 4 h and then reduced to dryness with a rotary evaporator. The residue was passed through an alumina column using a 100:1 (v/v) CH_2Cl_2–MeOH solution as the eluent. The first red-brown band was collected and reduced to dryness with a rotary evaporator, redissolved in a minimum amount of CH_2Cl_2, and precipitated by dropwise additon to Et_2O. The red-brown product was collected by vacuum filtration, washed with Et_2O and air dried; yield 0.051 g (0.039 mmol); 43% (Calc. for $C_{61}H_{47}ClF_4N_3O_4P_2BRu·0.5H_2O$: C, 59.16; H, 3.91. Found: C, 59.13; H, 4.05%).

Results and discussion

Fig. 1 shows the general scheme for the synthesis of the *trans*-spanning ruthenium complex, *trans*-[Ru(Cl)(trpy)(C3SPAN)]$^+$, **6**. The synthesis is initiated by combining $RuCl_3$(trpy) with one protected phosphine ligand and a reducing agent to form the *trans*-[Ru(Cl)$_2$(trpy){$Ph_2PC_6H_4(CH_2OC_5H_9O)$-*p*}], **1**. Irradiation of the reaction mixture with light[47] converts **1** to *cis*-[Ru(Cl)$_2$(trpy){$Ph_2PC_6H_4(CH_2OC_5H_9O)$-*p*}], **2**. The combination of excess phosphine with **2** produces *trans*-[Ru(Cl)(trpy)-{$Ph_2PC_6H_4(CH_2OC_5H_9O)$-*p*}$_2$][$PF_6$], **3**. Prior to the *trans*-spanning reaction, the phosphine groups are deprotected in an acid catalyzed step resulting in the formation of *trans*-[Ru(Cl)(trpy){$Ph_2PC_6H_4(CH_2OH)$-*p*}$_2$][PF_6], **4**. *trans*-Spanning is achieved by reacting **4** with an organic dioxychloride to give **6**, **7** or **8** in a double esterification reaction. The product is purified by column chromatography to isolate the monomeric species with yields of 40–60%. The use of a large volume of solvent during the spanning procedure prevents dimerization and/or oligimerization and increases the yields of the spanned complexes to values similar to those of the model reactions (*i.e.* the formation of dibenzyl adipate and dibenzyl glutarate).[48] Through the use of three different spans, –$(CH_2)_3$–, –$(CH_2)_4$– and –isophthalate–, we demonstrate that the *trans*-spanning linkage can be modified in terms of chain length and structure.

Electronic spectroscopy and cyclic voltammetric data

The UV-VIS spectroscopic and cyclic voltammetry data for the complexes are summarized in Table 2. Transitions at *ca.* 700, 550 and 400 nm in the *trans*-[Ru(Cl)$_2$(trpy)(PR_3)] complexes are assigned to Ru(dπ)→π*(trpy) metal-to-ligand charge transfer bands (MLCT) as observed for other *trans*-ruthenium complexes.[47,49–52] The transitions observed at 380, 330, 320, 286 and 275 nm are assigned to π→π* ligand (trpy, triphenylphosphine)-localized transitions.[47,53,54] These *trans*-(dichloro)-ruthenium complexes display one reversible couple assigned to the ruthenium(III/II) potential at approximately 0.50 V *vs*. SSCE in CH_2Cl_2.

The *cis*-[Ru(Cl)$_2$(trpy)(PR_3)] complexes are characterized by two MLCT transitions at *ca.* 530 and 490 nm. These wavelengths have shifted to shorter wavelengths relative to the *trans*-[Ru(Cl)$_2$(trpy)(PR_3)] complexes, however the absorbances maintain similar molar absorptivity values. The four ligand localized π→π* transitions occur at *ca*. 360, 320, 285 and 275 nm. These *cis*-(dichloro)ruthenium complexes display one reversible couple assigned to the ruthenium(III/II) potential at approximately 0.60 V *vs*. SSCE in CH_2Cl_2. The shifts to shorter wavelengths which accompany the increases in $E_{1/2}$ values are observed for other polypyridyl ruthenium complexes.[47,49–52,55,56] Both **1** and **2** have $E_{1/2}$ values which are 50 mV higher than the corresponding PPh_3 complexes. This increase in $E_{1/2}$ is consistent with the electron withdrawing nature of the protected group on the phosphine.

The addition of a second phosphine ligand to **2** and the consequent change from a neutral to a positively charged molecule result in a shift of the absorption maxima to higher energies. These absorbances are again assigned to MLCT bands from Ru(dπ)→ligand (π*) transitions. The absorption maxima of the complexes at 330, 310, 270, 230, and 210 nm are assigned to ligand localized π→π* transitions. Interestingly, the reversible ruthenium(III/II) redox couples for complexes **3**–**8** demonstrate a small range in $E_{1/2}$ values from +0.88 to +0.93 V *vs*. SSCE in CH_3CN and a linear relationship between the peak current ($i_{p,c}$) and the square root of the scan rate ($v^{1/2}$). This linear relationship indicates that the electron transfer is diffusion controlled

Table 2 UV-VIS spectroscopic and cyclic voltammetry data for selected ruthenium complexes

Complex[a]	$E_{\frac{1}{2}}$/V *vs.* SSCE	λ_{max}/nm ($10^{-3}\varepsilon$/cm^{-1} M^{-1})
trans-[Ru(Cl)$_2$(trpy)(PPh$_3$)]	+0.46[e]	705 (sh), 549(4.66), 403(4.71), 375 (sh), 331(17.9), 320 (sh), 286 (sh), 275(16.5)
trans-[Ru(Cl)$_2$(trpy)(Ph$_2$PR)], **1**[b]	+0.51	701 (sh), 552(4.84), 403(4.86), 381 (sh), 331(20.5), 320 (sh), 286 (sh), 275(21.0)
cis-[Ru(Cl)$_2$(trpy)(PPh$_3$)]	+0.58[e]	531(4.79), 488 (sh), 363 (sh), 319(20.8), 286 (sh), 275(16.3)
cis-[Ru(Cl)$_2$(trpy)(Ph$_2$PR)], **2**[b]	+0.63	533(5.35), 488 (sh), 362 (sh), 319(22.9), 285 (sh), 276(17.9)
trans-[Ru(Cl)(trpy)(Ph$_2$PR)$_2$][PF$_6$], **3**[c]	+0.88	474(3.83), 431 (sh), 334 (sh), 310(29.8), 270(78.6), 236(62.0), 209(96.6)
trans-[Ru(Cl)(trpy)(Ph$_2$PR′)$_2$][PF$_6$], **4**[c,d]	+0.88	473(3.35), 431 (sh), 332 (sh), 311(22.2), 270(45.8), 231 (sh), 208(98.6)
trans-[Ru(Cl)(trpy)(PPh$_3$)$_2$][PF$_6$], **5**[c]	+0.90	473(3.62), 431 (sh), 330 (sh), 312(23.2), 268(43.2)
trans-[Ru(Cl)(trpy)(C3SPAN)][PF$_6$], **6**[c]	+0.92	473(3.50), 432 (sh), 334 (sh), 311(21.7), 271(38.5), 232(52.1)
trans-[Ru(Cl)(trpy)(C4SPAN)][PF$_6$], **7**[c]	+0.91	473(3.84), 432 (sh), 334 (sh), 311(21.4), 271(39.9), 231(51.0)
trans-[Ru(Cl)(trpy)(ISPAN)][PF$_6$], **8**[c]	+0.93	471(4.10), 432 (sh), 333 (sh), 311(25.0), 271(42.0), 233(75.6)

[a] Measured in methylene chloride unless otherwise stated. [b] R = $C_6H_4(CH_2OC_5H_9O)$-*p*. [c] Measured in acetonitrile. [d] R′ = $C_6H_4(CH_2OH)$-*p*. [e] From ref. 47.

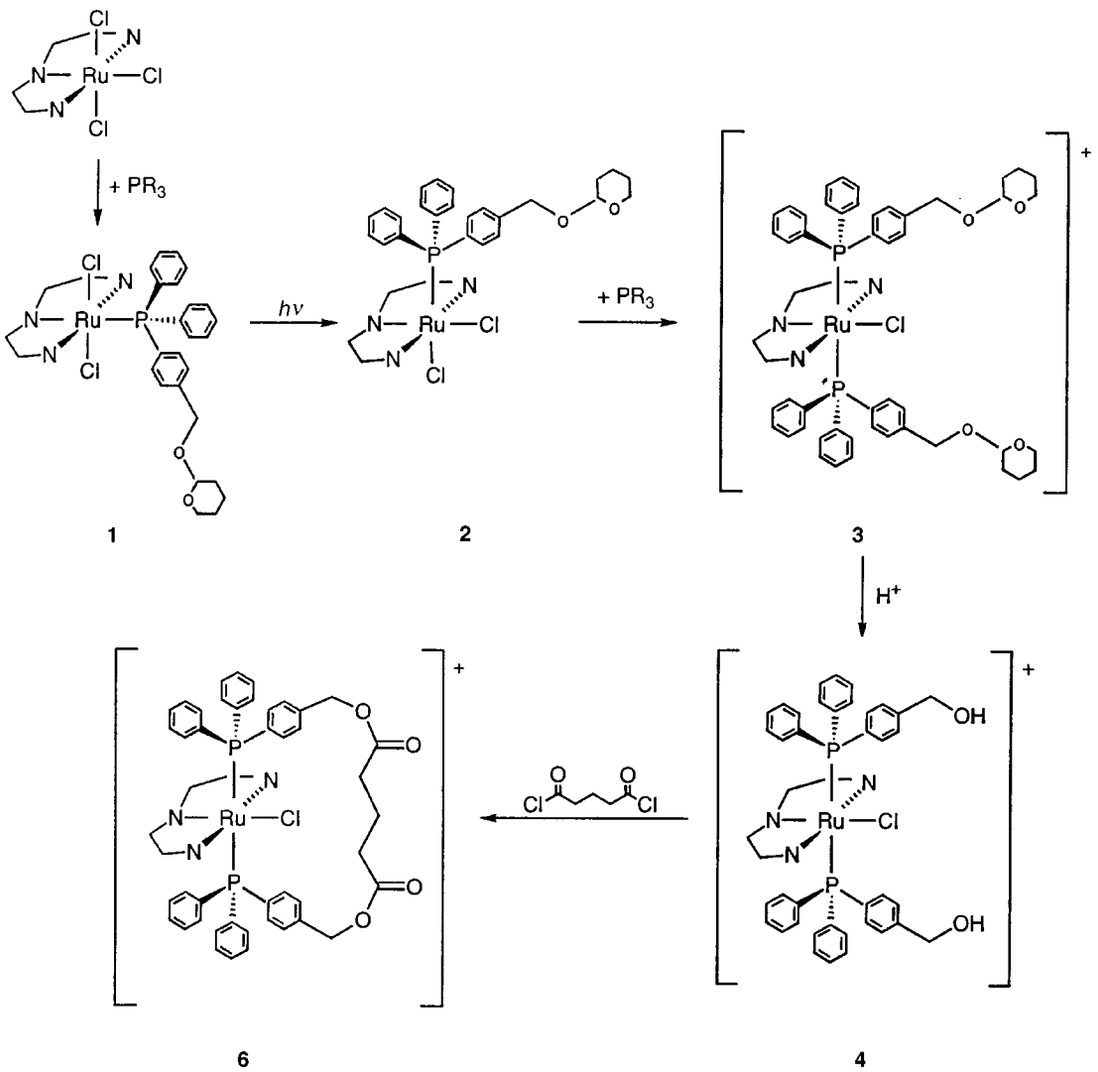

Fig. 1 The reaction scheme for the preparation of *trans*-[Ru(Cl)(trpy)(C3SPAN)]$^+$, **6**.

and is not influenced by the steric bulk of the spanning linkage (for complexes **6**–**8**). Finally, peak current ratios [cathodic peak current ($i_{p,c}$)/anodic peak current ($i_{p,a}$)], determined using the Nicholson Method,[57] ranged from 0.90–1.0 : 1 for all of the complexes used in this study. These data imply that electron transfer at the ruthenium metal center is reversible and that the ester linkages found in complexes **6**–**8** are stable to oxidation and reduction under standard electrochemical conditions. Thus, the ester linkage overcomes the disadvantages observed with the Takeuchi SL2 ligand (see above).

While changes in the electron donating or electron withdrawing nature of ligand substituents can result in variation of electronic properties at the metal center previous observations have also shown that the redox potential of a metal complex can change with steric ligand effects.[58–60] An advantage of the *in situ* ligand synthesis procedure is the ability to compare the span precursors to the spanned complexes. This comparison has enabled us to separate the electronic contributions from the steric contributions of the spanning linkage. This is most notable in light of studies involving the Venanzi preformed ligand SL1 complexes (see above),[19–26] where isolating the electronic effects of the spanning ligand from the steric effects caused by the strained geometries proved difficult.[21,24] The consistency of the spectroscopic and electrochemical data for the protected (**3**), deprotected (**4**), unsubstituted (**5**) and spanned (**6**–**8**) complexes indicates that changes in the periphery of the

Table 3 Selected interatomic distances (Å) and angles (°) for *trans*-[Ru(Cl)(trpy)(PPh_3)$_2$][BF_4]·CH_2Cl_2, **5**

(A) Ruthenium–ligand distances			
Ru(1)–P(1)	2.398(2)	Ru(1)–N(1)	2.098(6)
Ru(1)–P(2)	2.415(2)	Ru(1)–N(2)	1.964(7)
Ru(1)–Cl(1)	2.457(2)	Ru(1)–N(3)	2.072(6)
(B) Phosphorus–carbon distances			
P(1)–C(11)	1.841(8)	P(2)–C(41)	1.831(7)
P(1)–C(21)	1.831(8)	P(2)–C(51)	1.813(9)
P(1)–C(31)	1.847(8)	P(2)–C(61)	1.824(9)
(C) Distances within terpyridyl systems			
N(1)–C(71)	1.363(12)	N(3)–C(91)	1.350(10)
C(71)–C(72)	1.376(13)	C(91)–C(92)	1.377(12)
C(72)–C(73)	1.351(18)	C(92)–C(93)	1.397(15)
C(73)–C(74)	1.380(16)	C(93)–C(94)	1.356(14)
C(74)–C(75)	1.377(13)	C(94)–C(95)	1.383(13)
C(75)–N(1)	1.380(12)	C(95)–N(3)	1.357(11)
C(75)–C(81)	1.473(13)	C(85)–C(95)	1.476(12)
N(2)–C(81)	1.351(12)	C(83)–C(84)	1.390(16)
C(81)–C(82)	1.386(14)	C(84)–C(85)	1.376(12)
C(82)–C(83)	1.365(16)	C(85)–N(2)	1.357(11)
(D) Angles around the ruthenium atom			
P(1)–Ru(1)–P(2)	178.1(1)	P(1)–Ru(1)–Cl(1)	87.5(1)
P(2)–Ru(1)–Cl(1)	90.7(1)	P(1)–Ru(1)–N(1)	90.8(2)
P(2)–Ru(1)–N(1)	90.4(2)	Cl(1)–Ru(1)–N(1)	106.2(2)
P(1)–Ru(1)–N(2)	90.3(2)	P(2)–Ru(1)–N(2)	91.4(2)
Cl(1)–Ru(1)–N(2)	174.9(2)	N(1)–Ru(1)–N(2)	78.5(3)
P(1)–Ru(1)–N(3)	90.1(2)	P(2)–Ru(1)–N(3)	89.4(2)
Cl(1)–Ru(1)–N(3)	95.9(2)	N(1)–Ru(1)–N(3)	157.9(3)
N(2)–Ru(1)–N(3)	79.5(3)		
(E) Angles around phosphorus atoms			
Ru(1)–P(1)–C(11)	114.0(2)	C(11)–P(1)–C(21)	101.0(4)
Ru(1)–P(1)–C(21)	121.1(3)	C(11)–P(1)–C(31)	108.4(4)
Ru(1)–P(1)–C(31)	111.8(2)	C(21)–P(1)–C(31)	98.9(4)
Ru(1)–P(2)–C(41)	118.2(2)	C(41)–P(2)–C(51)	105.9(4)
Ru(1)–P(2)–C(51)	108.9(2)	C(41)–P(2)–C(61)	99.0(4)
Ru(1)–P(2)–C(61)	119.6(3)	C(51)–P(2)–C(61)	103.6(4)
(F) Angles at C_{ipso} in PPh_3 ligands			
C(16)–C(11)–C(12)	117.4(8)	C(46)–C(41)–C(42)	118.5(7)
C(26)–C(21)–C(22)	117.8(7)	C(56)–C(51)–C(52)	118.3(8)
C(36)–C(31)–C(32)	117.2(8)	C(66)–C(61)–C(62)	117.7(8)

ligand structure leave the electronic environment about the metal center relatively unchanged and implies that the geometry about the metal center is relatively undistorted from an ideal octahedral arrangement (this was later proven by X-ray crystallography, see below).

Conductivity analysis

Conductivity measurements were performed on **6** and **7** using the method of Feltham and Hayter.[61] The charge and nuclearity of the complexes were determined by measuring the equivalent conductivity (Λ_e) over a range of concentrations (expressed in terms of equivalent concentration, c). The data are obtained as Λ_o, the conductance at infinite dilution and B, the slope of the plot of ($\Lambda_o - \Lambda_e$) *versus* the square root of c. The use of equivalent concentrations in this technique eliminates the uncertainty in concentrations of complexes with unknown nuclearity and it allows for the differentiation of complexes having the same empirical formula but different molecular weight. The B values were 297 and 373 for **6** and **7** respectively, and are consistent with the values proposed by Davies for monomeric complexes with a 1:1 electrolyte in acetonitrile,[62] and by Leising for monomeric *trans*-diphosphine ruthenium(II) complexes and for ruthenium(II) complexes containing the Takeuchi SL2 spanning linkages.[38,50]

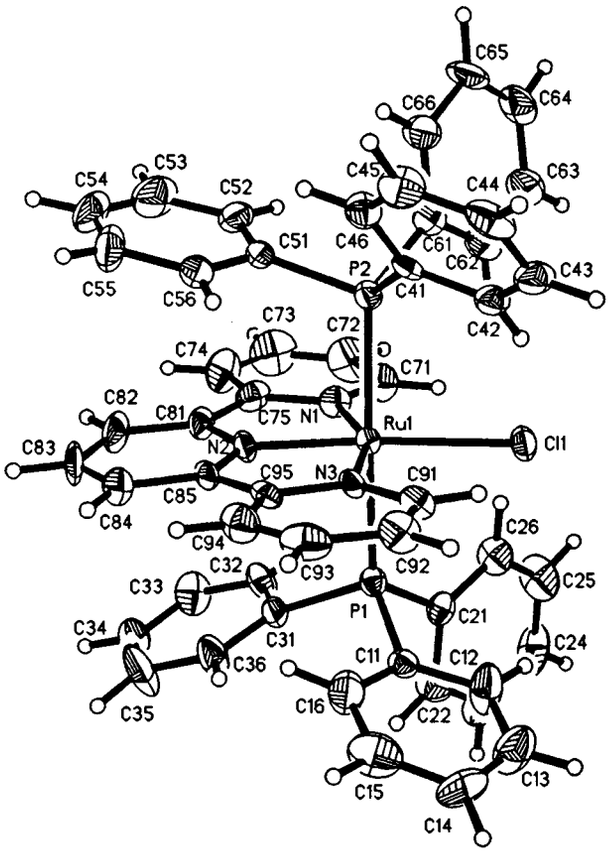

Fig. 2 ORTEP diagram of the *trans*-[Ru(Cl)(trpy)(PPh_3)$_2$]$^+$ cation, **5**.

Crystal structure analysis

Crystals of **5** were grown using the double vial diffusion technique in a CH_2Cl_2–toluene solution and crystallize with CH_2Cl_2 molecules in the lattice. Crystallographic-grade crystals of **7** were grown, after purification by column chromatography, from a solution of 12 mg complex–0.5 ml chloroform at approximately 18 °C. Selected bond distances and bond angles for **5** and **7** are listed in Tables 3 and 4 respectively. Crystals of **7** contain a disordered array of C_6H_5Me and CH_2Cl_2 molecules of crystallization about the inversion center at 1/2 1/2 0. Fig. 2 and 3 give perspective views and numbering schemes for **5** and **7** respectively.

The crystal structures of **5** and **7** are compared to determine whether distortions are brought about by the presence of the *trans*-spanning linkage. The crystal structures of **5** and **7** consist of arrays of ordered ruthenium cations and anions (BF_4^- for **5** and PF_6^- for **7**) in a 1:1 stoichiometry along with solvent of crystallization. Results of the structural analyses indicate that **5** adopts a C_{2v} geometry, while **7** adopts a C_1 geometry due to the position of the spanning ligand. One of the most significant aspects of the crystal structure of **7** is that the complex is monomeric, confirming the conductivity studies.

Both complexes show small distortions from an ideal octahedral geometry. First, the N(trpy terminal pyridine)–Ru–N(trpy terminal pyridine) bond angle for **5** is 157.9(3)° and for **7** is 157.7(2)°. These deviations are attributed to the geometrical constraints of the trpy backbone.[63] These angles differ greatly from those of the free trpy ligand at 128°,[64] however, they are within the range [156.9(5)–158.3(3)°] observed for other ruthenium(II) complexes.[50–52,65,66] The Ru–N(central trpy) bond length is 1.964(7) and 1.955(5) Å for **5** and **7** respectively; both structures show some dissymmetry in the Ru–N(trpy terminal pyridines) bond distances.

Comparisons between complexes containing two triphenylphosphine ligands and other *trans*-spanning ligands have been made in the literature. For example, the crystal structures of

Table 4 Interatomic distances (Å) and angles (°) for *trans*-[Ru(Cl)(trpy)(C4SPAN)][PF_6]·0.25C_6H_5Me·0.5CH_2Cl_2 **7**

(A) Ruthenium–ligand distances

Ru(1)–P(1)	2.397(2)	Ru(1)–N(71)	2.073(5)
Ru(1)–P(2)	2.397(2)	Ru(1)–N(81)	1.955(5)
Ru(1)–Cl(1)	2.481(2)	Ru(1)–N(91)	2.126(6)

(B) Phosphorus–carbon distances

P(1)–C(11)	1.836(8)	P(2)–C(41)	1.852(6)
P(1)–C(21)	1.831(7)	P(2)–C(51)	1.839(6)
P(1)–C(31)	1.825(6)	P(2)–C(61)	1.817(9)

(C) Distances within $PPh_2(C_6H_4)$ moieties

C(11)–C(12)	1.380(11)	C(11)–C(16)	1.395(9)
C(12)–C(13)	1.385(12)	C(13)–C(14)	1.375(9)
C(14)–C(15)	1.371(12)	C(15)–C(16)	1.384(14)
C(21)–C(22)	1.392(8)	C(21)–C(26)	1.387(10)
C(22)–C(23)	1.379(12)	C(23)–C(24)	1.356(12)
C(24)–C(25)	1.381(11)	C(25)–C(26)	1.388(13)
C(31)–C(32)	1.379(9)	C(31)–C(36)	1.392(11)
C(32)–C(33)	1.386(10)	C(33)–C(34)	1.361(13)
C(34)–C(35)	1.390(11)	C(35)–C(36)	1.376(10)
C(41)–C(42)	1.371(9)	C(41)–C(46)	1.397(12)
C(42)–C(43)	1.387(10)	C(43)–C(44)	1.375(12)
C(44)–C(45)	1.373(10)	C(45)–C(46)	1.384(9)
C(51)–C(52)	1.364(9)	C(51)–C(56)	1.373(10)
C(52)–C(53)	1.364(10)	C(53)–C(54)	1.362(13)
C(54)–C(55)	1.368(11)	C(55)–C(56)	1.385(10)
C(61)–C(62)	1.387(9)	C(61)–C(66)	1.420(11)
C(62)–C(63)	1.398(13)	C(63)–C(64)	1.372(14)
C(64)–C(65)	1.371(12)	C(65)–C(66)	1.379(16)

(D) Distances within the *trans*-spanning bridge

C(1)–O(2)	1.451(9)	C(1)–C(14)	1.507(12)
O(2)–C(3)	1.324(10)	C(3)–C(4)	1.512(10)
C(4)–C(5)	1.524(12)	C(5)–C(6)	1.481(14)
C(6)–C(7)	1.511(12)	C(7)–C(8)	1.512(14)
C(8)–O(9)	1.325(10)	O(9)–C(10)	1.436(11)
C(10)–C(44)	1.501(10)		

(E) Distances within carbonyl groups

C(3)–O(3)	1.204(9)	C(8)–O(8)	1.188(9)

(F) Angles around the ruthenium atom

P(1)–Ru(1)–P(2)	175.0(1)	P(1)–Ru(1)–Cl(1)	87.1(1)
P(2)–Ru(1)–Cl(1)	87.9(1)	P(1)–Ru(1)–N(71)	88.5(2)
P(2)–Ru(1)–N(71)	91.2(2)	Cl(1)–Ru(1)–N(71)	95.5(2)
P(1)–Ru(1)–N(81)	93.6(2)	P(2)–Ru(1)–N(81)	91.3(2)
Cl(1)–Ru(1)–N(81)	174.7(2)	N(71)–Ru(1)–N(81)	79.3(2)
P(1)–Ru(1)–N(91)	92.7(2)	P(2)–Ru(1)–N(91)	89.5(2)
Cl(1)–Ru(1)–N(91)	106.8(2)	N(71)–Ru(1)–N(91)	157.7(2)
N(81)–Ru(1)–N(91)	78.4(2)		

(G) Angles around phosphorus atoms

Ru(1)–P(1)–C(11)	114.4(2)	C(11)–P(1)–C(21)	108.0(3)
Ru(1)–P(1)–C(21)	110.6(3)	C(11)–P(1)–C(31)	101.4(3)
Ru(1)–P(1)–C(31)	119.7(2)	C(21)–P(1)–C(31)	101.5(3)
Ru(1)–P(2)–C(41)	112.9(2)	C(41)–P(2)–C(51)	99.7(3)
Ru(1)–P(2)–C(51)	120.7(2)	C(41)–P(2)–C(61)	107.9(3)
Ru(1)–P(2)–C(61)	111.5(2)	C(51)–P(2)–C(61)	102.7(3)

(H) Angles at C_{ipso} in PPh_3 ligands

C(16)–C(11)–C(12)	116.6(7)	C(46)–C(41)–C(42)	118.7(6)
C(26)–C(21)–C(22)	117.9(7)	C(56)–C(51)–C(52)	118.2(6)
C(36)–C(31)–C(32)	117.5(6)	C(66)–C(61)–C(62)	117.8(8)

(I) Angles within *trans*-spanning bridge

O(2)–C(1)–C(14)	110.7(8)	O(9)–C(10)–C(44)	106.6(6)
C(1)–O(2)–C(3)	116.8(6)	C(7)–C(8)–O(9)	111.6(7)
O(2)–C(3)–C(4)	110.0(6)	C(8)–O(9)–C(10)	117.0(6)
C(3)–C(4)–C(5)	115.6(6)	C(4)–C(5)–C(6)	115.3(8)
C(5)–C(6)–C(7)	114.3(8)	C(6)–C(7)–C(8)	116.5(8)

(J) Angles about carbonyl groups

O(2)–C(3)–O(3)	125.8(7)	O(3)–C(3)–C(4)	124.2(8)
C(7)–C(8)–O(8)	125.3(8)	O(8)–C(8)–C(9)	123.1(8)

Au(SL1)Cl[20,67] and $Au(PPh_3)_2Cl$[68] have significantly different P–Au–P bond angles [140.7(1)° and 132.1(1)° respectively]; as do CuCl(SL1)[67] and $CuBr(PPh_3)_2$[69] [at 131.9° and 126.0(1)°, respectively]. These data imply that the rigid spacer ligand, SL1, may be better at enforcing linear *trans*-geometries than two monodentate PPh_3 ligands. However, the latter differences must be interpreted with caution, especially in light of the significant changes in P–Ag–P bond angle that occur with change in anion.[20,24]

The P–Ru–P angles in both **5** and **7** deviate slightly from linearity (180°). Complex **5** has a P–Ru–P bond angle of 178.1(1)° while **7** has a P–Ru–P bond angle of 175.0(1)°. Although the P–Ru–P bond angle in **7** is smaller than in **5**, and could indicate strain on the octahedral geometry due to the spanning ligand, an investigation of *trans*-diphosphine-(terpyridyl)ruthenium(II) complexes which contain PMe_3,[50] PEt_3,[51] PPr_3[66] or PPh_3[65] ligands shows that P–Ru–P bond angles normally range between 175.1(1) and 178.2(2)°. Thus, the P–Ru–P bond angle observed in **7** is probably not caused by the spanning linkage. The P–Ru–P bond axis for both **5** and **7** appears to bend in the direction of the chloride ligand, implying that this region has less steric crowding than the region around the trpy ligand.

The diagrams of **5** and **7** show that the phosphine ligands align in a similar fashion over and under the trpy ligand. That is, for both structures one phenyl ring of the phosphine is parallel to the central pyridine ring of trpy; a second phenyl ring is orthogonal to the plane of the trpy ligand; and a third phenyl group of the phosphine is tilted from the terminal pyridine of the trpy ligand. The Ru–P bond distances in both complexes fall within the expected range found for other phosphine ruthenium complexes, which is 2.26–2.41 Å.[50–52,64–66] Such bond lengths are also similar to those observed with other metals and spanning linkages, for example [Ir(Cl)(CO)(SL1)][22] has an Ir–P bond length of 2.310(4) Å and $[Ir(Cl)_3(CO)(SL1)]$[22] has an average Ir–P bond length of 2.411 Å.

The Cl–Ru–N(central pyridine) bond angles are also less than the ideal 180° for both complexes: 174.9(2)° for **5** and 174.7(2)° for **7**. The phenyl groups of the phosphines that are oriented orthogonal to the trpy plane appear to push the chloride ligand in the opposite direction and expand the Cl–Ru–N(trpy terminal pyridine) bond angle to 106.2(2)° in **5** and 106.8(2)° for **7**. These angles are 10.3° and 11.3° greater than the second Cl–Ru–N(trpy terminal pyridine), *i.e.* where the phenyl group of the phosphine is approximately parallel to the terminal pyridine ring. This variation in bond angle is significant in light of other ligand (nitro or aqua)–Ru–N(trpy terminal pyridine) angles which vary between 99.6 and 102.5°.[50,51,65,66] The Ru–N(trpy terminal pyridine) bonds are different by 0.026 Å in **5** and by 0.053 Å for **7**. Also, the Ru–Cl bond distance in **7** is 0.024 Å longer than the Ru–Cl bond distance in **5**.

NMR spectroscopy

^1H and ^{13}C NMR spectroscopies were used to confirm the structures of the low spin, d^6, ruthenium(II) complexes and to investigate the effects of the *trans*-spanning linkages. The chemical shifts and coupling constants for all of the compounds are given in Table 5 (^1H NMR) and Table 6 (^{13}C NMR).

Analysis of the free trpy spectra. In 1971, Carlson *et al.* assigned the ^1H NMR spectrum of free trpy by drawing an analogy between trpy and 2,2′-bipyridine (bpy).[70] Assignments for bpy had previously been made by Castellano *et al.*[71] Our analysis of the ^1H NMR spectrum of the free trpy ligand differs from that reported by Carlson *et al.*[70] in our assignment of the

Table 5 ^{1}H NMR spectroscopy for ruthenium complexes

Complex[a]	δ (ppm) (integration, multiplicity,[b] coupling/Hz, *assignment*[c])
trpy	7.35 (2 H, ddd, J_{ba} = 4.8, J_{bc} = 7.5, J_{bd} = 1.2, *b*), 7.88 (2 H, ddd, J_{cd} = 8.0, J_{cb} = 7.5, J_{ca} = 1.8, *c*), 7.96 (1 H, t, J_{hg} = 8.0, *h*), 8.47 (2 H, d, J_{gh} = 8.0, *g*), 8.63 (2 H, dt, J_{dc} = 8.0, *d*), 8.69 (2 H, ddd, J_{ab} = 4.8, J_{db} = 1.2, J_{da} = 1.0, *a*)
trans-[Ru(Cl)(trpy)(PPh_3)$_2$][PF_6], **5**	7.08 (12 H, cm, *k*), 7.11[d] (2 H, —[e], J_{ba} = 5.4, J_{bc} = 7.4, J_{bd}[e], *b*), 7.14[d] (12 H, cm, *j*), 7.24 (6 H, cm, *l*), 7.47 (3 H, s, J_{gh}[e], *g* and *h*), 7.69 (2 H, td, J_{ca} = 1.3, J_{cb} = 7.4, J_{cd} = 8.2, *c*), 7.75 (2 H, dd, J_{dc} = 8.2, J_{db} = 1.6, J_{da}[e], *d*), 9.01 (2 H, d, J_{ab} = 5.4, J_{ac} = 1.3, J_{ad}[e], *a*)
trans-[Ru(Cl)(trpy)(C3SPAN)][PF_6], **6**	2.09 (2 H, p, *t*), 2.71 (4 H, t, *s*), 4.90 (4 H, s, *q*), 6.17 (4 H, bs, *n*), 6.77 (4 H, bd, J_{on} = 7.7, *o*), 7.10 (2 H, bt, J_{ba} = 5.8, J_{bc} = 7.6, J_{bd}[e], *b*), 7.22 (8 H, cm, *k*), 7.29[f] (2 H,[e], J_{gh} = 8.0, *g*), 7.30 (4 H, cm, *l*), 7.49 (1 H, t, J_{hg} = 8.0, *h*), 7.58 (2 H, d, J_{da}[e], J_{db}[e], J_{dc} = 8.1, *d*), 7.67 (10 H, td, J_{ca} = 1.2, J_{cb} = 7.6, J_{cd} = 8.1, *c* and *j*), 8.99 (2 H, bs, J_{ab} = 5.8, J_{ac} = 1.2, J_{ad}[e], *a*)
trans-[Ru(Cl)(trpy)(C4SPAN)][PF_6], **7**	1.81 (4 H, cm, *t*), 2.56 (4 H, cm, *s*), 4.88 (4 H, s, *q*), 6.24 (4 H, cm, *n*), 6.80 (4 H, bd, *o*), 7.11 (2 H, ddd, J_{ba} = 5.6, J_{bc} = 7.3, J_{bd} = 1.7, *b*), 7.21 (8 H, cm, *k*), 7.30 (4 H, cm, *l*), 7.35 (2 H, d, J_{gh} = 7.3, *g*), 7.44 (1 H, cm, J_{hg} = 7.3, *h*), 7.60 (2 H, d, J_{da}[e], J_{db} = 1.7, J_{dc} = 8.2, *d*), 7.60 (8 H, cm, *j*), 7.67 (2 H, td, J_{ca} = 1.3, J_{cb} = 7.3, J_{cd} = 8.2, *c*), 9.00 (2 H, bd, J_{ab} = 5.6, J_{ac} = 1.3, J_{ad}[e], *a*)
trans-[Ru(Cl)(trpy)(ISPAN)][PF_6], **8**	4.99 (4 H, s, *q*), 5.83 (4 H, p, *n*), 6.66 (4 H, bd, *o*), 7.10 (2 H, ddd, J_{ba} = 5.3, J_{bc} = 6.7, J_{bd} = 2.2, *b*), 7.22[d] (8 H, cm, *k*), 7.23[d] (4 H, cm, *l*), 7.49 (2 H, dd, J_{da} = 1.7, J_{db} = 2.2, J_{dc} = 8.5, *d*), 7.44 (3 H, bs, *g* and *h*), 7.54 (2 H, cm, J_{ca} = 1.2, J_{cb} = 6.7, J_{cd} = 8.5, *c*), 7.66 (1 H, t, J_{ut} = 7.9, *u*), 7.92 (8 H, cm, *j*), 8.37 (2 H, dd, J_{tu} = 7.9, J_{tv} = 1.6, *t*), 8.50 (1 H, bt, J_{vt} = 1.6, *v*), 9.20 (2 H, bd, J_{ab} = 5.3, J_{ac} = 1.2, J_{ad} = 1.7, *a*).

[a] NMR spectra were measured in CD_2Cl_2 and referenced against $CDHCl_2$. [b] Abbreviations: s = singlet, d = doublet, t = triplet, p = pentuplet, bs = broad singlet, bd = broad doublet, bt = broad triplet, dd = doublet of doublets, dt = doublet of triplets, td = triplet of doublets, ddd = doublet of doublet of doublets, cm = complex multiplet. [c] Letters used in assignments correlate to trpy Fig. 4; **5** Fig. 5; **6** Fig. 6; **7** Fig. 7; **8** Fig. 8. [d] Shift determined from corrected HETCOR data. [e] Could not determine due to overlap or broad linewidth. [f] Shift determined by COSY.

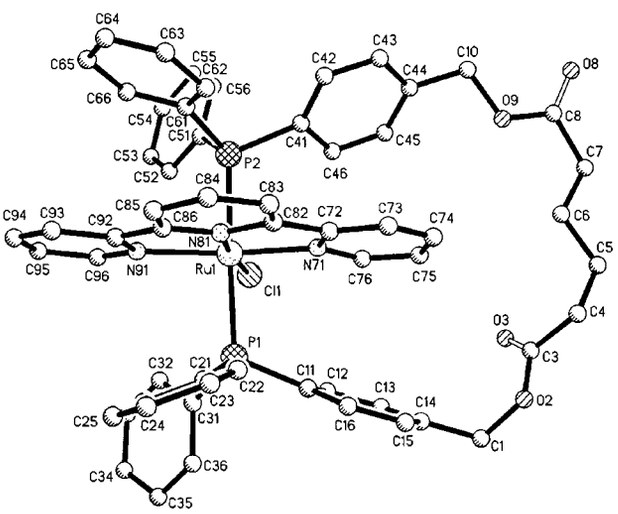

Fig. 3 Molecular geometry of the *trans*-[Ru(Cl)(C4SPAN)(trpy)]$^+$ cation, **7**. Hydrogen atoms are omitted for clarity.

chemical shifts for the H_d and H_g protons (see Fig. 4). The terminal pyridine rings in trpy are magnetically equivalent and have the first order sub-spectrum of a 2-substituted pyridine while the middle ring has the first order sub-spectrum of a 2,6-disubstituted pyridine. Free trpy demonstrates a *trans*,*trans*-configuration both in solution[63] and in the solid state[64] due to the repulsion of the non-bonding electrons on the nitrogen atoms. This has consequences for the proton chemical shifts. Protons H_a, H_b, H_c and H_h in free trpy have shifts similar to the equivalent positions in pyridine. However, H_d and H_g are shifted over 1 ppm downfield from their position in pyridine due to their interaction with the non-bonding electron pairs on the adjacent pyridine rings. The two-dimensional COSY spectrum (see SUP 57568, Fig. 9) of free trpy is consistent with our current assignments. Notably, J_{ab} is about half the size of J_{cd} for both free trpy and for trpy contained in complexes **5**–**8**. When this information is used in conjunction with the carbon shifts determined by HETCOR spectroscopy, confirmation of the proton assignments in the ruthenium complexes is possible.

The proton decoupled ^{13}C NMR resonances for free trpy are assigned (Fig. 4) based on one-bond HETCOR experiments (SUP 57568, Fig. 10) except in the case of C_e and C_f which are assigned based on N-bond HETCOR experiments. The ^{13}C NMR resonances for free trpy are within 0.3 to 2.5 ppm of the literature values for the resonances of free pyridine ($C_{ortho\ to\ N}$ δ 149.8, $C_{meta\ to\ N}$ δ 123.6 and $C_{para\ to\ N}$ δ 135.7)[72] except for C_e and C_f which are shifted by 6.7 and 5.9 ppm downfield, respectively, due to substituent effects.

Analysis of triphenylphosphine spectra. The ^{1}H NMR spectrum of free triphenylphosphine (PPh_3) shows one broad singlet in the aromatic region, δ 7.28 in $CDCl_3$.[73] The ^{13}C NMR spectrum of free PPh_3 shows seven peaks at δ 137.27, 137.12, 133.79, 133.53, 128.60, 128.44 and 128.35 in $CDCl_3$.[73]

NMR studies have been successful in characterizing the dynamic processes of PPh_3 ligands in many transition metal complexes.[74–77] Coordinated PPh_3 is capable of rotating about the three P–C_{ipso} bonds as well as as the metal–P bond. For steric reasons, the three phenyl groups generally adopt a chiral propeller-like conformation with either a clockwise or anti-clockwise screw configuration.[77] Interconversion of the two enantiomeric configurations or full rotation about any P–C_{ipso} bond requires cooperative motion within PPh_3.[78] In a conformational study of free triphenylphosphine, Brock and Ibers[78] estimated both of these barriers to rotation to be less than 2 kcal mol^{-1}. For [Fe(η^5-C_5H_5)(CO)(PPh_3)(COMe)], Davies determined that the P–Fe rotational activation energy barrier ($\Delta G^{\ddagger}$) was 10.3 kcal mol^{-1} and that the phenyl ring rotation about the P–C_{ipso} was rapid on the NMR time scale down to −90 °C.[77] In order to determine if the steric effects of the *trans*-spanning linkage resulted in restricted rotation of the phosphine ligand we employed (see below) variable temperature NMR studies on ruthenium complexes which contain phosphine ligands.

Analysis of the ruthenium complex spectra. The literature contains little information on the NMR behavior of *trans*-spanning complexes due at times to the difficulties associated with the separation of isomers (*cis* and *trans*, monomers and dimers) and also the insolubility of many of the complexes in common NMR solvents.[21] In contrast, the *trans*-spanning complexes **6**–**8** are monomeric, *trans*-isomers and are soluble in a variety of common NMR solvents. The ^{1}H and ^{13}C spectra of **6**, **7** and **8** are shown in Fig. 6–8 [HETCOR and COSY data are given in SUP 57568, Fig. 15, 16 (complex **6**), 19, 20 (**7**), and 23, 24 (**8**); variable temperature data are also given in SUP 57568, Figs.

Table 6 ^{13}C NMR spectroscopy for ruthenium complexes

Complex[a]	δ (ppm)[b] (coupling/Hz, *assignment*[c])
trpy	121.10[c] (*b*), 121.20[c] (*g*), 121.24[c] (*d*), 137.1[c] (*c*), 138.2[c] (*h*), 149.5[c] (*a*), 155.7[d] (*f*), 156.5[d] (*e*)
trans-[Ru(Cl)(trpy)(PPh_3)$_2$][PF_6], **5**	122.66 (*g*), 122.83 (*d*), 126.84 (*b*), 128.57 ($\lvert {}^3J_{PCk} + {}^5J_{P'Ck}\rvert$ = 9.1, *k*), 130.10 ($\lvert {}^4J_{PCl} + {}^6J_{PCl}\rvert$ = 1.6, *l*), 130.13 ($\lvert {}^1J_{PCi} + {}^3J_{P'Ci}\rvert$ = 39.2, *i*), 132.52 (s, *h*), 133.23 ($\lvert {}^2J_{PCj} + {}^4J_{P'Cj}\rvert$ = 10.3, *j*), 136.87 (*c*), 155.79 (*a*), 157.66 (*f*), 158.18 (*e*)
trans-[Ru(Cl)(trpy)(C3SPAN)][PF_6], **6**	20.72 (*t*), 33.07 (*s*), 66.40 (*q*), 122.74 (*g*), 122.76 (*d*), 127.17 (*b*), 128.75 ($\lvert {}^3J_{PCk} + {}^5J_{P'Ck}\rvert$ = 9.6, *k*), 129.74 ($\lvert {}^1J_{PCm} + {}^3J_{P'Cm}\rvert$ = 36.9, *m*), 129.85 ($\lvert {}^3J_{PCo} + {}^5J_{P'Co}\rvert$ = 7.7, *o*), 130.64 ($\lvert {}^4J_{PCl} + {}^6J_{P'Cl}\rvert$ = 1.9, *l*), 130.96 (2 C, $\lvert {}^2J_{PCn} + {}^4J_{P'Cn}\rvert$ = 8.6, *n*; $\lvert {}^1J_{PCi} + {}^3J_{P'Cl}\rvert$ = 41.0, *i*), 132.45 (*h*), 134.15 ($\lvert {}^2J_{PCj} + {}^4J_{P'Cj}\rvert$ = 10.8, *j*), 136.75 (*c*), 137.21 ($\lvert {}^4J_{PCp} + {}^6J_{P'Cp}\rvert$ = 1.9, *p*), 155.45 (*a*), 157.37 (*f*), 157.97 (*e*), 172.91 (*r*)
trans-[Ru(Cl)(trpy)(C4SPAN)][PF_6], **7**	24.67 (*t*), 34.17 (*s*), 66.00 (*q*), 122.55 (*d*), 122.64 (*g*), 127.08 (*b*), 128.67 ($\lvert {}^3J_{PCk} + {}^5J_{P'Ck}\rvert$ = 9.8, *k*), 128.73 ($\lvert {}^3J_{PCo} + {}^5J)_{P'Co}\rvert$ = 7.2, *o*), 128.94 ($\lvert {}^1J_{PCm} + {}^3J_{P'Cm}\rvert$ = 36.4, *m*), 130.51 ($\lvert {}^4J_{PCl} + {}^6J_{P'Cl}\rvert$ = 0.0, *l*), 130.82 ($\lvert {}^1J_{PCi} + {}^3J_{P'Ci}\rvert$ = 41.4, *i*), 131.13 ($\lvert {}^2J_{PCn} + {}^4J_{P'Cn}\rvert$ = 10.3, *n*), 132.32 (*h*), 134.07 ($\lvert {}^2J_{PCj} + {}^4J_{P'Cj}\rvert$ = 11.0, *j*), 136.73 (*c*), 137.94 ($\lvert {}^4J_{PCp} + {}^6J_{P'Cp}\rvert$ = 0.0, *p*), 155.54 (*a*), 157.43 (*f*), 157.87 (*e*), 173.26 (*r*)
trans-[Ru(Cl)(trpy)(ISPAN)][PF_6], **8**	68.38 (*q*), 122.91 (*d*), 123.31 (*g*), 126.96 (*b*), 127.28 (*v*), 128.80 ($\lvert {}^3J_{PCk} + {}^5J_{P'Ck}\rvert$ = 9.7, *k*), 129.40 ($\lvert {}^1J_{PCm} + {}^3J_{P'Cm}\rvert$ = 36.0, *m*), 130.08 (*u*), 130.78 ($\lvert {}^4J_{PCl} + {}^6J_{P'Cl}\rvert$ = 0.0, *l*), 130.84 ($\lvert {}^1J_{PCi} + {}^3J_{P'Ci}\rvert$ = 40.9, *i*), 130.89 ($\lvert {}^2J_{PCn} + {}^4J_{P'Cn}\rvert$ = 8.7, *n*), 130.90 (*s*), 131.03 ($\lvert {}^3J_{PCo} + {}^5J_{P'Co}\rvert$ = 7.4, *o*), 132.40 (*h*), 134.24 ($\lvert {}^2J_{PCj} + {}^4J_{P'Cj}\rvert$ = 11.0, *j*), 135.59 (*t*), 135.70 ($\lvert {}^4J_{PCp} + {}^6J_{P'Cp}\rvert$ = 0.0, *p*), 136.82 (*c*), 155.78 (*a*), 156.82 (*f*), 158.22 (*e*), 165.65 (*r*)

[a] NMR spectra were measured in CD_2Cl_2 and referenced against $CDHCl_2$. [b] Letters used in assignments correlate to trpy Fig. 4; **5** Fig. 5; **6** Fig. 6; **7** Fig. 7; **8** Fig. 8. [c] Determined by one-bond HETCOR. [d] Determined by N-bond HETCOR.

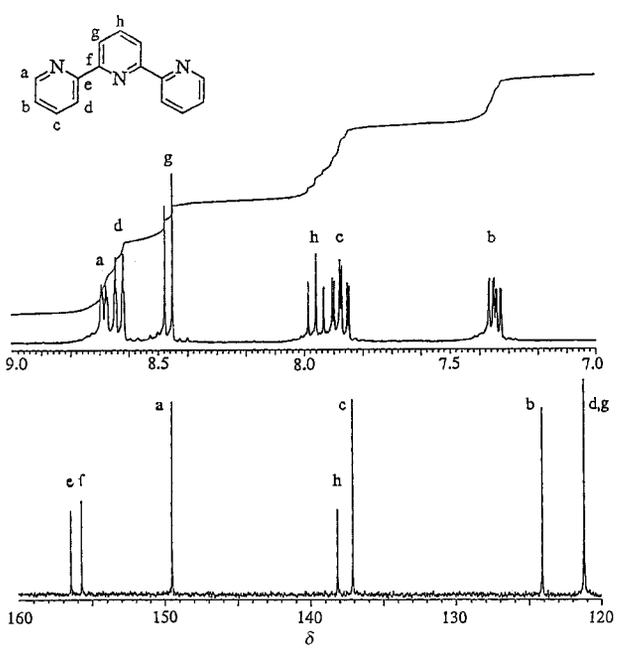

Fig. 4 ^1H and ^{13}C NMR spectra (300 MHz) of 2,2′ : 6′,6″-terpyridine (trpy) in methylene chloride-d_2.

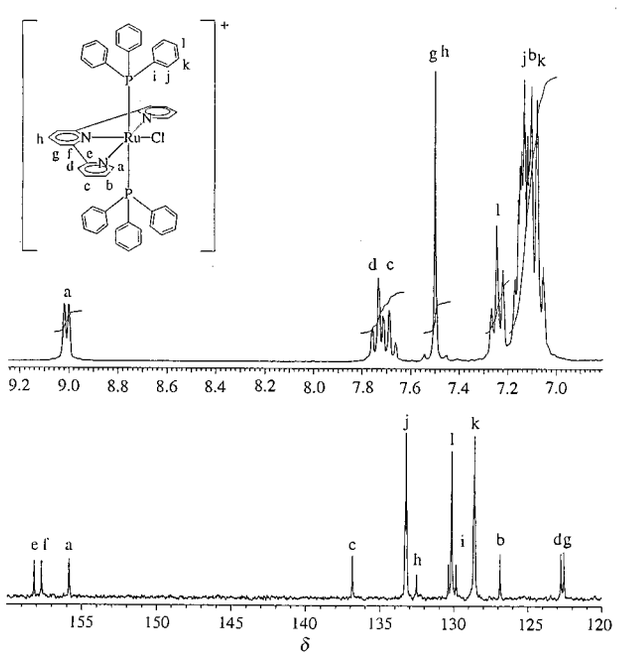

Fig. 5 ^1H and ^{13}C NMR spectra (300 MHz) of *trans*-[Ru(Cl)(trpy)-(PPh_3)$_2$]$^+$, **5** in methylene chloride-d_2.

17, 18 (complex **6**), and 21, 22 (complex **7**)]. Room temperature spectra will be the subject of discussion below unless otherwise noted.

I. Analysis of coordinated trpy spectra. The coordination of the trpy ligand to a ruthenium(II) cation can result in a downfield shift of the bonded trpy proton resonances relative to free trpy;[50,70] however, while H_a moves downfield 0.30–0.51 ppm in **5**–**8** as expected, the chemical shifts of the other trpy protons in **5**–**8** move 0.19–1.18 ppm upfield relative to the free trpy ligand. A possible reason for the downfield shift of H_a is given below. The ^{13}C NMR chemical shifts of bonded trpy in **5** (Fig. 5) vary little when compared with the free trpy resonances with the following exceptions: C_a is 6.3 ppm and C_b is 5.7 ppm downfield of the free trpy positions, while the chemical shift of C_h in **5** is 5.7 ppm upfield of that in free trpy. Similar changes in chemical shifts are observed for **6**–**8**.

II. Analysis of the coordinated phosphine ligand spectrum for 5. The proton chemical shifts of the triphenylphosphine ligands of **5** are assigned as complex multiplets: *meta* (H_k, δ 7.08), *ortho* (H_j, δ 7.14) and *para* (H_l, δ 7.24). When compared to the free triphenylphosphine ligand, the chemical shifts of **5** are 0.04–0.21 ppm upfield of their expected position. Thus, there seems to be a mutual anisotropic deshielding between the phenyl rings and the trpy ligand. These results can be explained for **5** if the possible motions of the triphenylphosphine groups are considered.

As only three proton resonances are observed for the PPh_3 moieties of **5**, free rotation about all three P–C_{ipso} bonds as well as the Ru–P bond is indicated. The ORTEP diagram of **5** (Fig. 2) shows that (a) each phenyl group of triphenylphosphine has a different orientation depending on its position relative to the trpy ligand and (b) both PPh_3 ligands are similarly arranged. Two phenyl rings are located over and under the central pyridine ring of trpy in an essentially parallel arrangement. The other two pairs of phenyl rings are positioned on each side of the trpy ligand and are nearly perpendicular to the plane of the terminal trpy pyridines. Thus, from the crystal structure it may be postulated that as each triphenylphosphine rotates along the Ru–P bond each phenyl ring will adjust its orientation along the P–C_{ipso} axis. That is, as each phenyl ring moves around the Ru–P bond, it may travel a monotonic or slightly oscillatory path over the trpy ring, but, as it clears the plane above (or

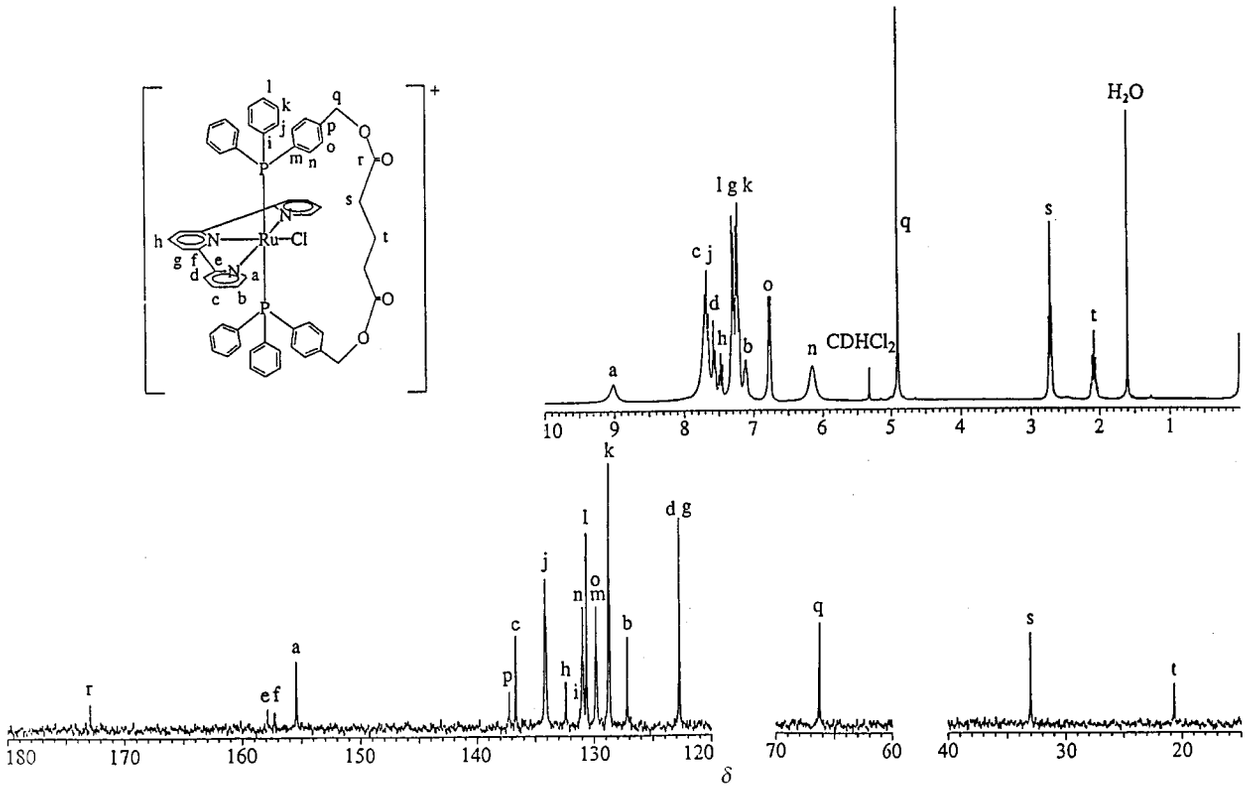

Fig. 6 ^{1}H and ^{13}C NMR spectra (300 MHz) of *trans*-[Ru(Cl)(trpy)(C3SPAN)]$^{+}$, **6** in methylene chloride-d_2.

below) the trpy ligand, it may rotate about the P–C_{ipso} bond to become perpendicular to the trpy ring thereby time averaging the *ortho* and *meta* proton resonances and resulting in only three unique proton resonances.

If this model is correct, the chemical shifts of the PPh_3 ligands are expected to be upfield relative to the free PPh_3, since the PPh_3 ligands of **5** spend more time in the shielding areas over the trpy compared to the two pockets between the chlorine and each of the terminal pyridines of trpy. Likewise the trpy protons of **5** (except for H_a) should experience shielding by the phenyl rings of the PPh_3 ligands and should also be found upfield when compared to the free trpy ligand. As these general upfield shifts are indeed observed in both the PPh_3 and trpy ligands, anisotropic deshielding may be the cause. Notably, the H_a protons are expected to be unique since the phenyl rings of the PPh_3 may freely rotate once they clear the plane of the trpy ligand. The 0.3 ppm downfield shift for H_a of **5** may be due to anisotropic deshielding from the phenyls in the pockets.

The triphenylphosphine ligands in the ^{13}C NMR spectrum of **5** show a set of four triplets, although that from the *para* position, C_l, looks like a singlet at low resolution. The signals are triplets due to virtual coupling to the second phosphorus. Since the two-bond P–Ru–P′ coupling is much larger than the P–C couplings, the high order pattern is a triplet rather than a doublet-of-doublets or a pentuplet. One can then measure only the algebraic sum of the two P–C couplings across the outer line of the triplet. For **5** the values are *ipso* ($|^{1}J_{P-Ci} + {}^{3}J_{P-Ci}|$ = 39.2 Hz), *ortho* ($|^{2}J_{P-Cj} + {}^{4}J_{P-Cj}|$ = 10.3 Hz), *meta* ($|^{3}J_{P-Ck} + {}^{5}J_{P-Ck}|$ = 9.1 Hz) and *para* ($|^{4}J_{P-Cl} + {}^{6}J_{P-Cl}|$ = 1.6 Hz). The peak assignments for **5** have been corroborated through HETCOR and COSY experiments.

III. Analysis of the coordinated phosphine ligand spectra for ***6–8***. Proton shifts for the phenyl groups of PPh_3 show some changes on going from **5** to the span complexes, **6–8**. First, complexes **6–8** show a sub-spectrum for a *para*-disubstituted phenyl ring in the aromatic region as part of the spanning linkage and **8** shows an additional 1,3-disubstituted phenyl pattern for the isophthalate linkage. For any given phenyl ring on the phosphine ligand, the two *ortho* positions are equivalent to each other as are the two *meta* positions. These results indicate that the phenyl rings are undergoing rapid rotation about the P–C_{ipso} bond at room temperature. Second, *meta* and *para* protons maintain similar chemical shift values for **5–8** but there are significant differences between the complexes in the positions of the *ortho* protons of the phenyl rings, H_j. The H_j chemical shifts of **6** and **7** are approx. 0.5 ppm downfield relative to **5**; while the chemical shift of H_j in **8** is 0.78 ppm downfield relative to **5**. These downfield shifts will be discussed below in terms of motional averaging in the span complexes. Finally, the 0.3 ppm downfield shift for H_a of **6–8** may also be attributed to the anisotropic deshielding from the phenyls in the pockets. There is little difference in the ^{13}C shifts between the spanned complexes, **6–8**, and that containing the triphenylphosphine ligand, **5**.

IV. Analysis of the variable temperature spectra for ***5***. Restricted rotation about the P–C_{ipso} bonds or Ru–P bond should be observed if the phosphine ligands are sterically confined; variable temperature studies were conducted to detect such restricted rotations. If the rotation about each P–C_{ipso} becomes slow on cooling, it is expected that the *ortho* and *meta* peaks of the triphenylphosphine moiety will split into two distinct resonances while the *ipso* (^{13}C only) and *para* resonances should remain singular. If rotation about the Ru–P bond becomes slow on the NMR time scale, the peaks observed from the *ipso*, *ortho*, *meta* and *para* carbons should split into three, one for each of the rotating phenyl groups. Variable temperature ^{1}H and ^{13}C NMR spectra for **5** (see SUP 57568, Fig. 13 and 14) show no line broadenings until −90 °C where H_j, C_i and C_j show significant broadening and C_l shows slight broadening. Since the *ipso* carbon, C_i and the *para* carbon, C_j, should not show broadening for slowed rotation about the P–C_{ipso} bond, it is possible but not conclusive that rotation about the P–Ru bond is becoming slow at low temperatures. Interestingly, [Fe(η^5-C_5H_5)(CO)(PPh_3)(COMe)] shows a similar pattern of low temperature behavior in the ^{13}C spectrum.[77] For the iron complex, the *ipso*, *ortho* and *para* carbons show broadening at

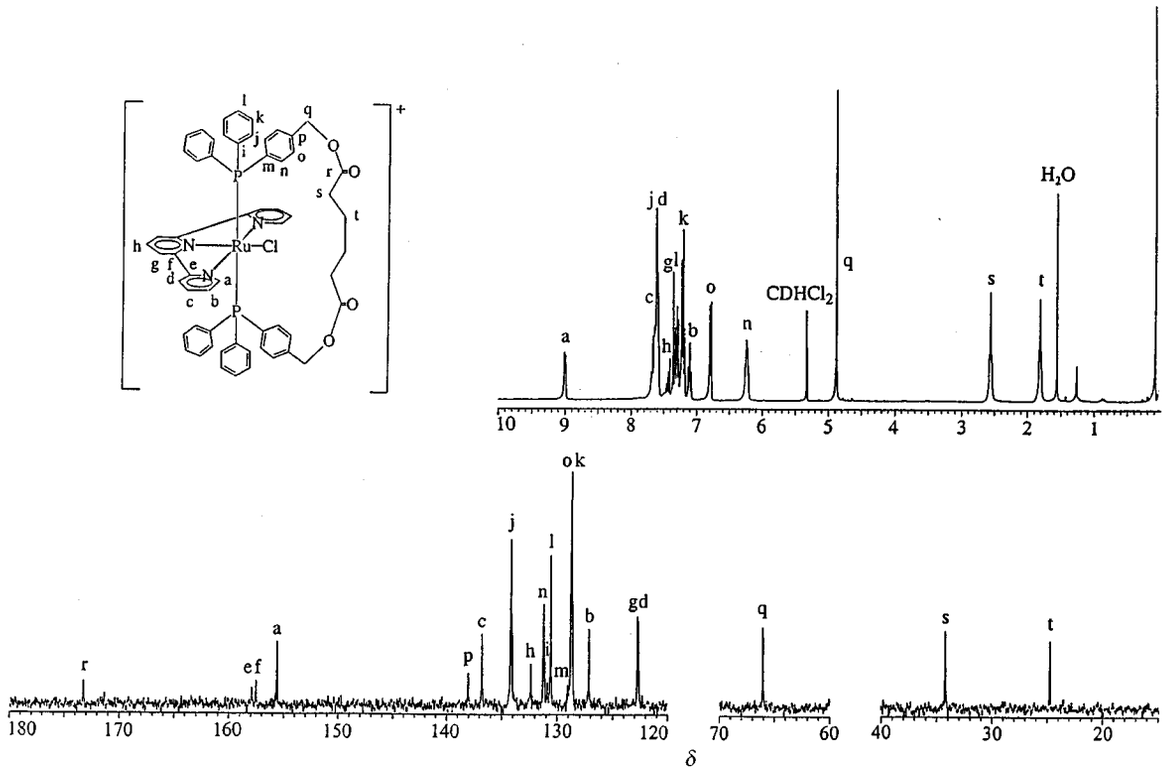

Fig. 7 ^{1}H and ^{13}C NMR spectra (300 MHz) of *trans*-[Ru(Cl)(trpy)(C4SPAN)]$^{+}$, **7** in methylene chloride-d_2.

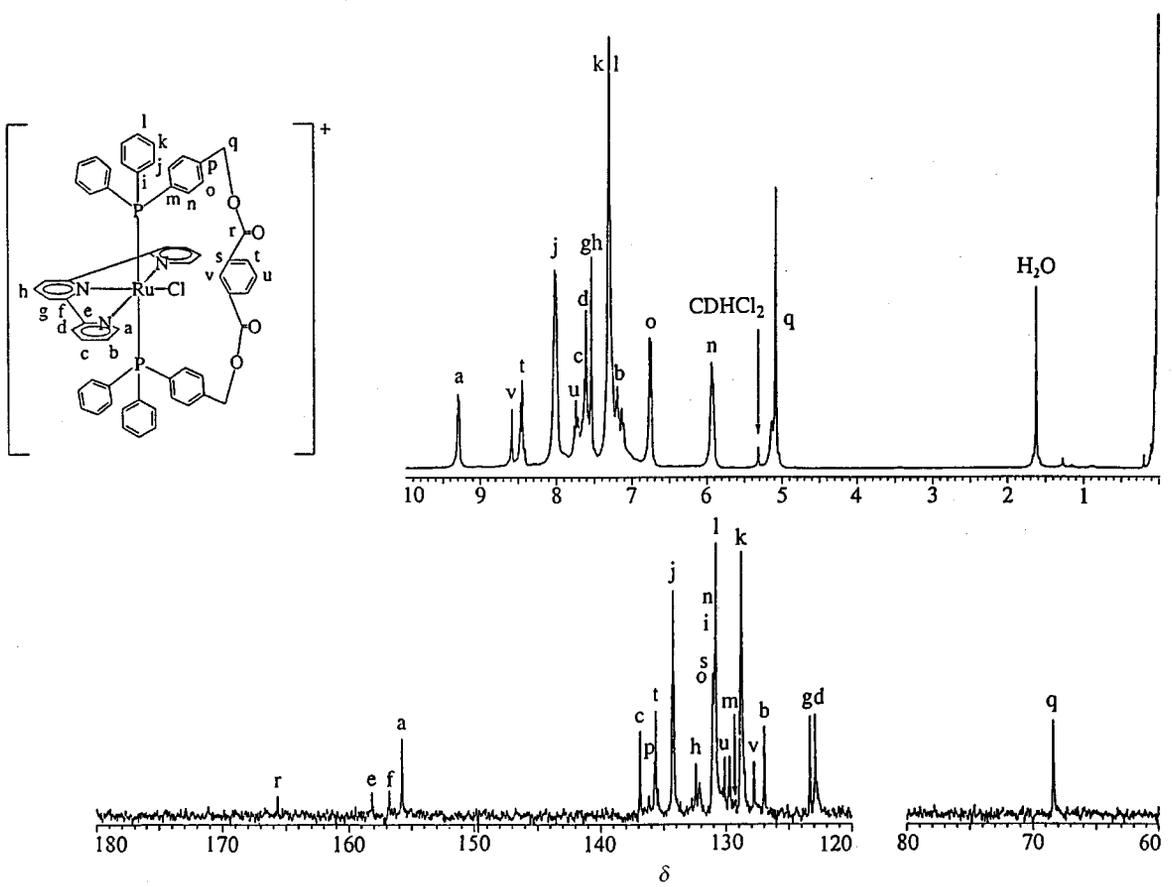

Fig. 8 ^{1}H and ^{13}C NMR spectra (300 MHz) of *trans*-[Ru(Cl)(trpy)(ISPAN)]$^{+}$, **8** in methylene chloride-d_2.

−60 °C with complete freezing out of the spectrum at −90 °C. The *meta* carbons are only starting to broaden at −90 °C and there is no sign of broadening for the acetyl methyl group or the cyclopentadienyl ring. For [Fe(η^5-C_5H_5)(CO)(PPh_3)(COMe)], Davies determined an experimental $\Delta G = 10$ kcal mol^{-1} for the Fe–P rotation at 62.90 MHz. As **5** requires a lower temperature for the start of broadening, even at a higher frequency (75 MHz), the Ru–P rotation in **5** is faster.

V. Analysis of the variable temperature spectra for ***6*****–*****8***. The variable temperature NMR spectra of **6** and **7** are qualitatively

similar to that of **5** except that even though there is no sign of broadening for the trpy resonances of **5** at −90 °C, the H_a, H_j and H_n resonances of **6** and **7** are already broad at room temperature. Maximum line broadenings for H_a, H_j, H_n and H_o are found between 5 °C and −40 °C. Below −40 °C these resonances sharpen though they do not split into separate resonances as described above for slowed rotations about the Ru–P or P–C_{ipso} bonds. At −60 °C, these resonances are sharp indicating that the motions about the Ru–P and P–C_{ipso} bonds are still fast on the NMR time scale. At −90 °C, H_a, H_j and H_n start to broaden but again, there is no indication of which motion is slowing. The methylene proton signals for the span also broaden but it is not possible to tell if this is an independent conformational process in the spanning linkage or if this is related to rotation about the P–Ru bond.

Complex **7** follows the same behavior as **6** but maximum coalescence starts about 40 °C lower. Complex **7** is expected to be more accommodating than **6** for rotation about either the trpy or chloride moieties. The difference in the coalescence temperatures may be related to subtle changes in span rotation about the P–Ru bond.

Finally, two types of motion appear to be available in the spanned complexes. The first involves a complete 360° rotation of the span about the P–Ru–P axis, where the span passes over both the chloride and the meridional trpy ligand. The second involves a restricted "fan-like" motion of the spanning linkage limited by the two terminal pyridines of the trpy ligands, where the span passes over only the chloride ligand and not the trpy ligand. Both mechanisms would time average the trpy resonances. At this time, it is not possible to distinguish which of these motional mechanisms is operating.

Conclusions

The *in situ* strategy for the preparation of *trans*-spanning ligands with ester linkages resulted in spanning linkages which are stable to oxidation and reduction, hydrolysis and cyclometallation while maintaining the benefits of span variability and the formation of ruthenium complexes which display bond angles close to ideal octahedral geometry. The NMR spectral analyses yielded several observations: (1) the original assignment of the ^{1}H NMR spectrum of trpy by Carlson is inconsistent with our COSY and HETCOR analyses, (2) the NMR spectra of **6**–**8** are consistent with a flexible spanning linkage that does not demonstrate restricted rotation about either the P–C_{ipso} or the Ru–P bonds even at low temperatures, and (3) maximal coalescence increased with temperature with shorter alkyl chain lengths in the *trans*-spanning linkage. Finally, the X-ray crystal structure analysis of **7** showed that the spanning linkage is positioned in one of the two pockets defined by the chloride ligand and the terminal pyridine groups of trpy.

Acknowledgements

This work was supported in part by the National Science Foundation (CHE 9120602) and the ARCO Chemical Company. Purchase of the Siemens R3m/v diffractometer was made possible by Grant 89-13733 from the Chemical Instrumentation Program of the National Science Foundation. The authors also gratefully acknowledge Johnson Matthey/Alfa/Aesar for the loan of the $RuCl_3 \cdot nH_2O$ used in these experiments. The authors acknowledge the assistance of Mr Simit D. Shah, Mr Sejal C. Patel and Mr Brian M. Scull of Villanova University in preparation, purification and characterization of the complexes.

References

1 J. C. Bailar, Jr., *Coord. Chem. Rev.*, 1990, **100**, 1.
2 D. M. A. Minahan, W. E. Hill and C. A. McAuliffe, *Coord. Chem. Rev.*, 1984, **55**, 31.
3 A. Pryde, B. L. Shaw and B. Weeks, *J. Chem. Soc.*, *Dalton Trans.*, 1976, 322.
4 N. A. Al-Salem, H. D. Empsall, R. Markham, B. L. Shaw and B. Weeks, *J. Chem. Soc.*, *Dalton Trans.*, 1979, 1972.
5 C. Crocker, R. J. Errington, R. Markham, C. J. Moulton, K. J. Odell and B. L. Shaw, *J. Am. Chem. Soc.*, 1980, **102**, 4373.
6 B. L. Shaw, *J. Am. Chem. Soc.*, 1975, **97**, 3856.
7 A. Pryde, B. L. Shaw and B. Weeks, *J. Chem. Soc.*, *Dalton Trans.*, 1976, 322.
8 H. D. Empsall, E. Mentzer, D. Pawson, B. L. Shaw, R. Mason and G. A. Williams, *J. Chem. Soc.*, *Chem. Commun.*, 1977, 311.
9 F. C. Marsh, R. Mason, K. M. Thomas and B. L. Shaw, *J. Chem. Soc.*, *Chem. Commun.*, 1975, 584.
10 N. W. Alcock, J. M. Brown and J. C. Jeffrey, *J. Chem. Soc.*, *Chem. Commun.*, 1974, 829.
11 N. W. Alcock, J. M. Brown and J. C. Jeffrey, *J. Chem. Soc.*, *Dalton Trans.*, 1976, 583.
12 N. W. Alcock, J. M. Brown and J. C. Jeffrey, *J. Chem. Soc.*, *Dalton Trans.*, 1977, 888.
13 W. E. Hill, J. G. Taylor, C. A. McAuliffe, K. W. Muir and L. Manojlovic-Muir, *J. Chem. Soc.*, *Dalton Trans.*, 1982, 833.
14 W. E. Hill, C. A. McAuliffe, I. E. Niven and R. V. Parish, *Inorg. Chim. Acta*, 1979, **38**, 273.
15 W. Levason, C. A. McAuliffe and S. G. Murray, *J. Organomet. Chem.*, 1976, **110**, C25.
16 W. E. Hill, D. M. A. Minahan, J. G. Taylor and C. A. McAuliffe, *J. Am. Chem. Soc.*, 1982, **104**, 6001.
17 (*a*) W. E. Hill, D. M. A. Minahan, J. G. Taylor and C. A. McAuliffe, *J. Chem. Soc.*, *Perkin Trans. 2*, 1982, 327; (*b*) J. C. Briggs, C. A. McAuliffe, W. E. Hill, D. M. A. Minahan and G. Dyer, *J. Chem. Soc.*, *Dalton Trans.*, 1982, 321; (*c*) J. C. Briggs, C. A. McAuliffe, W. E. Hill, D. M. A. Minahan, J. G. Taylor and G. Dyer, *Inorg. Chem.*, 1982, **21**, 4204; (*d*) W. E. Hill, D. M. A. Minahan, C. A. McAuliffe and K. L. Minten, *Inorg. Chim. Acta*, 1983, **74**, 9; (*e*) W. E. Hill, D. M. A. Minahan and C. A. McAuliffe, *Inorg. Chem.*, 1983, **22**, 3382; (*f*) J. C. Briggs, C. A. McAuliffe and G. Dyer, *J. Chem. Soc.*, *Dalton Trans.*, 1984, 423; (*g*) W. E. Hill, M. Q. Islam, T. R. Webb and C. A. McAuliffe, *Inorg. Chim. Acta*, 1988, **146**, 111.
18 H. M. K. K. Pathirana, A. W. Downs, W. R. McWhinnie and P. Granger, *Inorg. Chim. Acta*, 1988, **143**, 161.
19 P. N. Kapoor, P. S. Pregosin and L. M. Venanzi, *Helv. Chim. Acta*, 1982, **65**, 654.
20 M. Barrow, H.-B. Bürgi, M. Camalli, F. Caruso, E. Fischer, L. M. Venanzi and L. Zambonelli, *Inorg. Chem.*, 1983, **22**, 2356.
21 L. I. Elding, B. Kellenberger and L. M. Venanzi, *Helv. Chim. Acta*, 1983, **66**, 1676.
22 E. Baumgartner, F. J. S. Reed, L. M. Venanzi, F. Bachechi, P. Mura and L. Zambonelli, *Helv. Chim. Acta*, 1983, **66**, 2572.
23 P. Boron-Rettore, D. M. Grove and L. M. Venanzi, *Helv. Chim. Acta*, 1984, **67**, 65.
24 M. Camalli, F. Caruso, S. Chaloupka and L. M. Venanzi, *Helv. Chim. Acta*, 1988, **71**, 703.
25 M. Camalli, F. Caruso, S. Chaloupka, P. N. Kapoor, P. S. Pregosin and L. M. Venanzi, *Helv. Chim. Acta*, 1984, **67**, 1603.
26 H.-B. Bürgi, J. Murray-Rust, M. Camalli, F. Caruso and L. M. Venanzi, *Helv. Chim. Acta*, 1989, **72**, 1293.
27 D. M. P. Mingos, D. J. Sherman and I. D. Williams, *Transition Met. Chem.*, 1987, **12**, 493.
28 C. Crocker, R. J. Errington, R. Markham, C. J. Moulton and B. L. Shaw, *J. Chem. Soc.*, *Dalton Trans.*, 1982, 387.
29 R. J. Errington and B. L. Shaw, *J. Organomet. Chem.*, 1982, **238**, 319.
30 S. D. Perera, M. Shamsuddin and B. L. Shaw, *Can. J. Chem.*, 1995, **73**, 1010.
31 J. R. Briggs, A. G. Constable, W. S. McDonald and B. L. Shaw, *J. Chem. Soc.*, *Dalton Trans.*, 1982, 1225.
32 H. Rimml and L. M. Venanzi, *J. Orgamomet. Chem.*, 1983, **259**, C6.
33 S. D. Perera, B. L. Shaw and M. Thornton-Pett, *J. Chem. Soc.*, *Dalton Trans.*, 1992, 1469.
34 S. D. Perera, B. L. Shaw and M. Thornton-Pett, *J. Chem. Soc.*, *Dalton Trans.*, 1994, 3311.
35 K. K. Hii, S. D. Perera and B. L. Shaw, *J. Chem. Soc.*, *Dalton Trans.*, 1995, 625.
36 C. Crocker, H. D. Empsall, R. J. Errington, E. M. Hyde, W. S. McDonald, R. Markham, M. C. Norton, B. L. Shaw and B. Weeks, *J. Chem. Soc.*, *Dalton Trans.*, 1982, 1217.
37 R. J. Errington, W. S. McDonald and B. L. Shaw, *J. Chem. Soc.*, *Dalton Trans.*, 1982, 1829.
38 R. A. Leising, J. J. Grzybowski and K. J. Takeuchi, *Inorg. Chem.*, 1988, **27**, 1020.
39 D. L. Jameson and L. E. Guise, *Tetrahedron Lett.*, 1991, **32**, 1989.

40 D. D. Perrin and W. L. F. Armarego, *Purification of Laboratory Chemicals*, Pergamon Press, Oxford, 3rd edn., 1988.
41 J. R. Garbow, D. P. Weitekamp and A. Pines, *Chem. Phys. Lett.*, 1982, **93**, 504.
42 G. E. Martin and A. S. Zektzer, *Magn. Reson. Chem.*, 1988, **26**, 631.
43 M. R. Churchill, R. A. Lashewycz and F. J. Rotella, *Inorg. Chem.*, 1977, **16**, 265.
44 G. M. Sheldrick, SHELXTL PLUS, Siemens Analytical Instruments, Madison, WI, 1983.
45 M. R. Churchill, *Inorg. Chem.*, 1973, **12**, 1213.
46 C. K. Johnson, ORTEP II, Report ORNL-5138, Oak Ridge National Laboratory, Oak Ridge, TN, 1974.
47 B. P. Sullivan, J. M. Calvert and T. J. Meyer, *Inorg. Chem.*, 1980, **19**, 1404.
48 B. S. Furness, A. J. Hannaford, P. W. G. Smith and A. R. Tatchell, in *Vogel's Textbook of Practical Organic Chemistry*, J. Wiley and Sons, New York, 5th edn., 1989.
49 R. A. Leising, S. A. Kubow and K. J. Takeuchi, *Inorg. Chem.*, 1990, **29**, 4569.
50 R. A. Leising, S. A. Kubow, M. R. Churchill, L. A. Buttrey, J. W. Ziller and K. J. Takeuchi, *Inorg. Chem.*, 1990, **29**, 1306.
51 H. J. Lawson, T. S. Janik, M. R. Churchill and K. J. Takeuchi, *Inorg. Chim. Acta*, 1990, **174**, 197.
52 L. F. Szczepura, S. A. Kubow, R. A. Leising, W. J. Perez, M. H. V. Huynh, C. H. Lake, D. G. Churchill, M. R. Churchill and K. J. Takeuchi, *J. Chem. Soc.*, *Dalton Trans.*, 1996, 1463.
53 R. P. Thummel and Y. Jahng, *J. Org. Chem.*, 1985, **50**, 2407.
54 K. Nakamoto, *J. Phys. Chem.*, 1960, **64**, 1420.
55 H. S. Lim, D. J. Barclay and F. C. Anson, *Inorg. Chem.*, 1972, **11**, 1460.
56 T. Matsubara and P. C. Ford, *Inorg. Chem.*, 1976, **15**, 1107.
57 R. S. Nicholson, *Anal. Chem.*, 1966, **38**, 1406.
58 C. A. Bessel, J. A. Margarucci, J. H. Acquaye, R. S. Rubino, J. Crandall, A. J. Jircitano and K. J. Takeuchi, *Inorg. Chem.*, 1993, **32**, 5779.
59 D. T. Walker and H. Taube, *Inorg. Chem.*, 1981, **20**, 2828.
60 D. A. Bohling, J. F. Evans and K. R. Mann, *Inorg. Chem.*, 1982, **21**, 3546.
61 R. D. Feltham and R. G. Hayter, *J. Chem. Soc.*, 1964, 4587.
62 J. A. Davies, F. R. Hartley and S. G. Murray, *Inorg. Chim. Acta*, 1980, **43**, 69.
63 E. Constable, *J. Chem. Soc.*, *Dalton Trans.*, 1985, 2687.
64 C. A. Bessel, R. F. See, D. J. Jameson, M. R. Churchill and K. J. Takeuchi, *J. Chem. Soc.*, *Dalton Trans.*, 1992, 3223.
65 M. R. Churchill, R.F. See, C. A. Bessel and K. J. Takeuchi, *J. Chem. Crystallogr.*, 1996, **26**, 853.
66 M. R. Churchill, L. Krajkowski, L. F. Szczepura and K. J. Takeuchi, *J. Chem. Crystallogr.*, 1996, **26**, 543.
67 M. Barrow, H.-B. Bürgi, D. K. Johnson and L. M. Venanzi, *J. Am. Chem. Soc.*, 1976, **98**, 2356.
68 N. C. Baezinger, K. M. Dittemore and J. R. Doyle, *Inorg. Chem.*, 1974, **13**, 805.
69 P. H. Davis, R. L. Belford and I. C. Paul, *Inorg. Chem.*, 1973, **12**, 213.
70 F. E. Lytle, L. M. Petrosky and L. R. Carlson, *Anal. Chim. Acta*, 1971, **57**, 239.
71 S. Castellano, H. Gunther and S. Ebersole, *J. Phys. Chem.*, 1965, **69**, 4166.
72 E. Pretsch, J. Seibl, W. Simon and T. Clerc, *Tables of Spectral Data for Structure Determination of Organic Compounds*, Springer-Verlag, New York, 1983.
73 C. J. Pouchert and J. Behnke, *Aldrich Library of ^{13}C and ^{1}H FT NMR Spectra*, Aldrich Chemical Company, Inc., Milwaukee, WI, 1st edn., 1993, vol. 2, p. 1653.
74 J. W. Faller and B. V. Johnson, *J. Organomet. Chem.*, 1975, **96**, 99.
75 J. Vicente, M.-T. Chicote, M.-C. Lagunas, P. G. Jones and B. Ahrens, *Inorg. Chem.*, 1997, **36**, 4938.
76 E. E. Wille, D. S. Stephenson, P. Capriel and G. Binsch, *J. Am. Chem. Soc.*, 1982, **104**, 405.
77 S. G. Davies, A. E. Derome and J. P. McNally, *J. Am. Chem. Soc.*, 1991, **113**, 2854 and refs. therein.
78 C. P. Brock and J. A. Ibers, *Acta Crystallogr.*, *Sect. B*, 1973, **29**, 2426.

Paper 8/07574C